

A&A manuscript no.

(will be inserted by hand later)

Your thesaurus codes are:

Section 3: Extragalactic astronomy (13.25.2; X-rays: galaxies, 11.01.2;
Galaxies: Seyfert, 11.09.1 IRAS 09104+4109)ASTRONOMY
AND
ASTROPHYSICS

BeppoSAX uncovers a type-2 QSO in the hyperluminous infrared galaxy IRAS 09104+4109

A. Franceschini¹, L. Bassani², M. Cappi², G.L. Granato³, G. Malaguti², E. Palazzi², M. Persic⁴¹ Dipartimento di Astronomia, Vicolo Osservatorio 5, I-35122 Padova, Italy; E-mail: franceschini@pd.astro.it² ITeSRE/CNR, via Gobetti 101, I-40129 Bologna, Italy³ Osservatorio Astronomico, Vicolo Osservatorio 5, I-35122 Padova, Italy⁴ Osservatorio Astronomico, Via G. Tiepolo 11, I-34131 Trieste, Italy

Received 15 July 1999/ Accepted 3 September 1999

Abstract. We studied with BeppoSAX the infrared luminous galaxy IRAS 09104+4109 over a very wide X-ray band from 0.1 to 80 keV. Our observations indicate the dominance of a thermal component at energies below 8 keV, which we attribute to the free-free emission from the intracluster (IC) plasma surrounding the source. Above 10 keV we find evidence for the existence of flux in excess with respect to the free-free IC plasma emission. This, together with the marginal detection of a neutral iron line at ~ 6.4 keV, gives a strong indication for the presence of an AGN deeply buried within the source. This component is best modelled by a strongly absorbed ($N_{\mathrm{H}} \geq 5 \times 10^{24} \text{ cm}^{-2}$) power-law plus unabsorbed reflection spectrum ($0.15 \leq R \leq 0.3$), which is also responsible for the cold iron line. The unabsorbed broad-band (2-100 keV) X-ray emission of this AGN is $2.5 \times 10^{46} \text{ erg s}^{-1}$, well within the range of quasar luminosities. Our results indicate that IRAS 09104+4109 is indeed the prototype of a rare class of sources, the luminous type-2 QSOs. The association of this source with a huge cooling-flow of $\sim 1000 M_{\odot}$ in the cluster, as indicated by the X-ray data, might suggest that such condition of extremely fast mass accumulation could favour the survival of a thick obscuring envelope, which would otherwise be quickly destroyed by the very luminous central source.

Key words: galaxies: individual:IRAS 09104+4109-
galaxies: active- X-rays: galaxies

1. Introduction

The nature of Hyperluminous Infrared Galaxies (HyLIRGs, i.e. sources with bolometric luminosity in excess of $10^{12} L_{\odot}$, mostly emitted in the mid/far-IR) has been the subject of a lively debate since their discovery by IRAS. Observations have been accumulated in recent years, but, in spite of recent significant progresses

based on mid/far-IR spectroscopy (Genzel et al. 1998), the origin of their high luminosity remains uncertain, with massive starbursts and AGN both suspected to be responsible for the huge observed flux. Although optical spectroscopic data often indicate the presence of an AGN in HyLIRGs, several of them have not been detected (yet) in X-rays (Ogasaka et al. 1997), so the idea that they harbour a powerful QSO is still to be verified. If the dominant radiation power is due to an AGN, this must be deeply buried within large amounts of absorbing material because these sources appear as underluminous in soft X-rays with respect to normal AGNs. Hard X-ray measurements (above 10 keV) are then particularly effective in probing the presence of an optically-hidden AGN, as they penetrate column densities as high as several $\times 10^{24} \text{ cm}^{-2}$. Testing this would bear relevant implications for the long sought high redshift/luminosity analogues of Seyfert-2 galaxies, which are required by the unified model of AGN, and for the origin of the X-ray and IR cosmic backgrounds.

Among HyLIRGs, certainly one of the most intriguing is IRAS 09104+4109 ($z=0.442$), which is the most luminous object in the Universe with $z < 0.5$ and one of the most luminous IR-galaxies known ($L_{\mathrm{FIR}} \sim 2 \times 10^{46} \text{ ergs}^{-1}$). Kleinmann et al. (1988) have shown it to have a Seyfert2-like spectrum, with strong narrow emission lines. Later Hines & Wills (1993) and Hines et al. (1999) reported the detection of broad MgII and Balmer emission lines in the highly polarized spectrum. Both near- and mid-IR spectroscopy of the source provided evidence for the presence of a dusty torus (Taniguchi et al. 1997, Evans et al. 1998); this was further confirmed by HST imaging polarimetry of the source (Hines et al. 1999). An ASCA observation of IRAS 09104+4109 revealed it as a powerful X-ray source, with a power law spectrum (photon index ~ 2) similar to what is observed in most AGNs and a strong line at 6.67 keV, interpreted as due to helium-like iron scattered into our line of sight (Fabian et al. 1994a). However, this is not an unequivocal interpretation of the

of galaxies, which also emits in X-rays. Indeed a follow-up ROSAT HRI image of this sky region confirmed that the X-ray emission is extended and dominated by a cooling flow (Fabian & Crawford 1995); given the similarity of the extrapolated ASCA flux to that found by ROSAT, it is likely that the bulk of the 0.1–10 keV emission is also dominated by radiation from the hot gas in the surrounding cluster and not by the AGN. In fact ASCA data were better remodelled by an isothermal gas and an absorbed cooling flow, although the strength of the iron line was such that a contribution from a hidden nucleus could not be excluded.

In this paper we report X-ray observations with BeppoSAX of IRAS 09103+4109, and in particular the detection of excess emission at energies greater than 10 keV, which is likely due to non-thermal quasar emission emerging from a thick absorbing torus, well in excess of the thermal emission from the cluster. We will argue that this may be the first high-luminosity type-2 QSO detected in X-rays.

In Sect. 2 we report about the observations and data reduction, while Sect. 3 expands on the analysis of the spectral data. Our results for the fitting of the 0.1–10 keV spectrum are reported in Sect. 4, and in Sect. 5 those for the higher energies. The very complex nature of this source revealed by BeppoSAX is discussed in Sect. 6. We assume $H_0 = 50$ km/s/Mpc throughout the paper.

2. Observation and data reduction

The BeppoSAX X-ray observatory (Boella et al. 1997a) is a major programme of the Italian Space Agency with participation of the Netherlands Agency for Aerospace Programs. This work concerns results obtained with three of the Narrow Field Instruments (NFI) onboard: the Low Energy Concentrator Spectrometer (LECS; Parmar et al. 1997), the Medium Energy Concentrator Spectrometers (MECS; Boella et al. 1997b), and with the Phoswich Detector System (PDS; Frontera et al. 1997). LECS, MECS and PDS operative energy bands are 0.1–4.5 keV, 1.5–10 keV and 13–80 keV, respectively. The data from the HPGSPC did not provide significant count rate and therefore will not be considered here.

BeppoSAX NFI pointed at IRAS P09104+4109 from Apr 18th, to Apr 19th, 1998. The reduction procedures and screening criteria used to produce the linearized and equalized (between the two MECS) event files of the LECS and MECS were standard (Guainazzi et al. 1999). PDS data were analyzed using the XAS reduction procedure which takes into account rise time and spike corrections (Chiappetti & Dal Fiume 1997). The effective on-source exposure times were 2.42×10^4 s for the LECS, 5.47×10^4 s for the MECS, and 3.43×10^4 s for the PDS. Spectral data were extracted from regions centred on IRAS 09104+4109 with radii of 2' and 4', matching the PSF FWHM, for

background subtraction was performed by means of blank sky spectra extracted from the region around the source.

The PDS products were obtained by plain subtraction of the "off-" from the "on-source" data. The net source count rates were $(1.53 \pm 0.09) \times 10^{-2}$ c/s in the LECS (0.1–4.5 keV), and $(1.72 \pm 0.05) \times 10^{-2}$ c/s in the two MECS (2–10 keV). The net source count rate in the PDS was 0.107 ± 0.026 c/s between 13 and 80 keV, which gives a detection at 3.3σ level also after a conservative subtraction of the systematic residuals which are currently evaluated at ~ 0.02 c/s in the 13–200 keV band (Guainazzi & Matteuzzi 1997).

3. Spectral analysis

LECS and MECS data were rebinned in order to sample the energy resolution of the detector with an accuracy proportional to the count rate: one channel for LECS and 5 channels for MECS. Spectral data from LECS, MECS and PDS have been fitted simultaneously. Normalization constants have been introduced to allow for known differences in the absolute cross-calibration between the detectors. The values of the two constants have been allowed to vary and turned out to be within $\sim 5\%$ of the suggested values (see Fiore et al. 1999). The spectral analysis has been performed by means of the XSPEC 10.0 package, and using the instrument response matrices released by the BeppoSAX Science Data Centre in September 1997. All quoted errors correspond to 90% confidence intervals (for one interesting parameter this corresponds to $\Delta\chi^2 = 2.71$). Source plus background light curves did not indicate significant flux variability. Therefore the data from the whole observation were summed together for the spectral analysis.

All the models used in what follows contain an additional term to allow for the absorption of X-rays due to our Galaxy, that in the direction of IRAS P09104+4109 amounts to 1.81×10^{20} cm $^{-2}$ (Murphy et al. 1996). Given the high z of the source, all the spectral parameters are given in the reference system of the emitting source unless otherwise specified.

4. The 0.1–10 keV spectrum

To check the consistency with previous X-ray data we first concentrate on the 0.1–10 keV band and fit the LECS-MECS data with an absorbed power law plus a narrow ($\sigma \equiv 0$) line to account for excess emission around 6–7 keV, as done by Fabian et al. (1994a) for ASCA data. The fit is satisfactory ($\chi^2/\nu = 48.1/60$) and results in a spectrum having a photon index $\Gamma = 1.9 \pm 0.1$ and an absorbing column density $N_H = (1.4^{+1.8}_{-0.9}) \times 10^{21}$ cm $^{-2}$; the line is centered at 6.62 ± 0.12 keV and has a rest frame equivalent width (EW) of 1026^{+365}_{-253} eV. If the line width is allowed to vary, the additional parameter gives only an 80% improve-

with a rest frame width of (0.3 ± 0.2) keV. These model parameters are in agreement with those determined by Fabian et al. (1994a) except for the line equivalent width, which is higher in the BeppoSAX observation compared with the ASCA one (444^{+120}_{-173} eV), but still consistent at 2σ level.

The unabsorbed rest frame luminosity in the 0.5-10 keV band is similar to the one determined by ASCA (1.9×10^{45} erg s $^{-1}$), indicating that the emission did not change over years. In view of this lack of variability and of the ROSAT resolved images of a diffuse IC source at low energies (Fabian & Crawford 1995), a more appropriate description of the 0.1-10 keV spectrum is in terms of thermal emission from the hot gas in the cluster surrounding the source. Consequently we have fitted the data both with a Bremsstrahlung model plus a gaussian line to parameterize the Fe line energy and intensity and with the XSPEC/MEKAL model to estimate the metal abundances¹.

A good fit is obtained in the first case ($\chi^2/\nu=47.3/61$) for a gas temperature of $kT=9.7^{+2.7}_{-1.8}$ keV and no absorption in excess of the Galactic value. The line energy and equivalent width are consistent with the values found with the power law model (6.63 ± 0.12 keV, $EW=920^{+362}_{-237}$ eV). Also in this case the line is compatible with zero width and so in the subsequent analysis the line was always assumed to be narrow.

The MEKAL model gives a best-fit temperature of $8.3^{+1.9}_{-1.5}$ keV and a metal abundance consistent with solar, i.e $Z \simeq 1.2 \pm 0.5 Z_\odot$ ($\chi^2/\nu=51.9/62$). This fit in count units and the corresponding residuals are reported in Fig. 1. According to the correlation found by Fabian et al. (1994b), however, this abundance is unusually high for the measured temperature, a better value being $Z \leq 0.4$ solar (in particular for a cluster at this large redshift), in which case kT becomes ≥ 9 keV. Also note that some residual emission is present around the iron line peak energy when using the MEKAL model (see Fig. 1). This explains the slightly better fit and lower line energy (compared with the expected 6.7 keV) obtained with the Bremsstrahlung model.

In view of these inconsistencies, we have added a narrow gaussian line to the MEKAL model: this extra line turned out to be centered at $6.1^{+0.4}_{-0.3}$ keV (rest-frame) and characterized by a rest-frame $EW=406^{+174}_{-316}$ eV with respect to the thermal continuum. The addition of this extra line provides an improvement of the fit ($\Delta\chi^2=5.2$ for two additional parameters) which is significant at more than 90% confidence level. Although the cold line is poorly constrained in the contour plot of the line energy versus

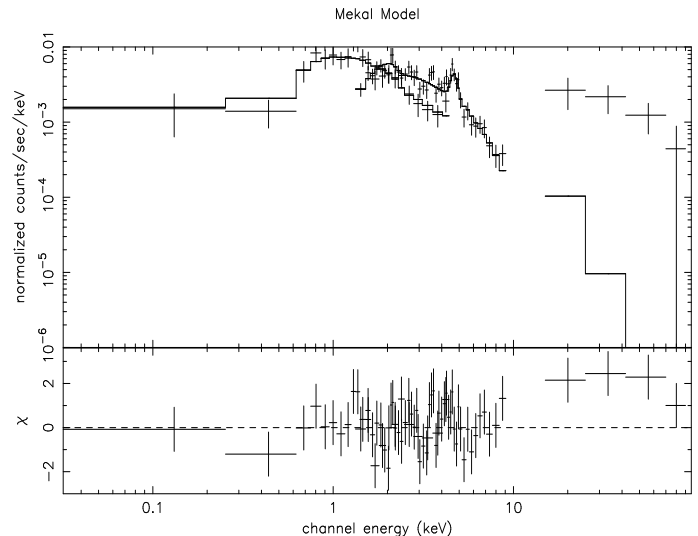


Fig. 1. BeppoSAX LECS, MECS and PDS data of IRAS 09104+4109 fitted with a MEKAL model (top panel). The residuals between the data and the model are plotted at the bottom with error bars.

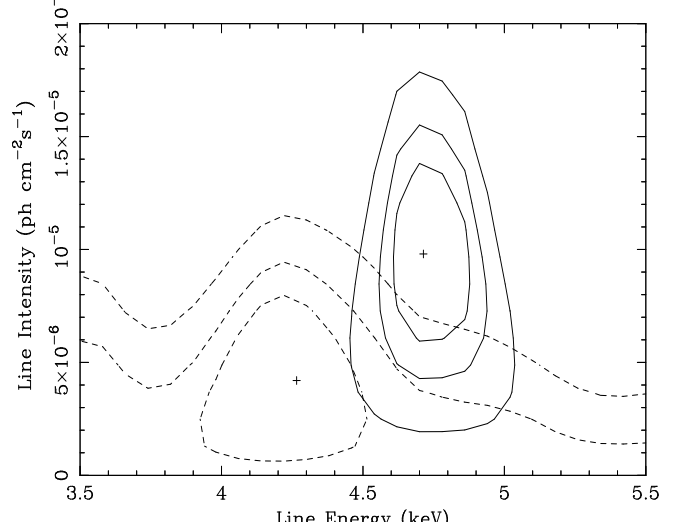


Fig. 2. Contour plot of line energy versus intensity for the 6.4 keV line (dashed line) and 6.7 keV line (continuous line) in the observer rest frame, assuming a Bremsstrahlung model. The best-fit EW (observer rest frame) are 78^{+204}_{-58} eV and 493^{+397}_{-302} eV for the cold and warm iron line respectively. The three contour levels correspond to 68%, 90% and 99% rejection probability.

normalization, it is however separated from the warm iron line at the 90% confidence level (see Fig. 2, where the line fitting is done using the Bremsstrahlung model).

Also note that when in the MEKAL model the iron abundance is fixed to 0.4, i.e. a value more appropriate for the cluster temperature observed, the 6.4 keV line becomes significant at more than 99% confidence and has an

¹ MEKAL is a program of the XSPEC library modeling the emission of a hot IC plasma (including free-free continuum, edge and line emission), as a function of the plasma temperature kT , ion and electron density, source redshift z , and average

We have also tried to add an absorbed cooling flow to the MEKAL model (as done by Fabian & Crawford 1995 with the ASCA data) but found that this extra component was not required by the data: the quality of the fit does not improve and the mass cooling rate is poorly constrained ($\leq 1520 M_{\odot} \text{ yr}^{-1}$).

In conclusion, the LECS-MECS data basically confirm previous X-ray results (Fabian et al. 1994a; Fabian & Crawford 1995) and give a further indication that the bulk of the 0.1 to 10 keV emission is dominated by the cluster thermal component. We do not find strong evidence at these energies neither for a cooling flow nor for quasar emission. However, the marginal detection of a neutral iron line already suggests the presence of an AGN, although providing a minor contribution to the continuum at these energies.

5. The AGN nucleus uncovered by the PDS

Extrapolation of the best fit MEKAL model discussed above fails to reproduce the higher energy PDS data, indicating the existence of excess emission above 10 keV (see Fig. 1). However, given the large field of view of the PDS (1.3° FWHM) care must be taken to check that no hard X-ray emitting sources could be present in the target field and contaminate the PDS signal. Inspection of the ~ 45 arcminutes diameter mapped by the SAX NFI reveals the presence of 5 marginal ($S/N > 3$) sources in the 0.1-2 keV energy channel, none of which is present in the highest energy map at 5-10 keV. So no high-energy sources, apart from IRAS 09104+4109, are indicated in the inner PDS field. Further inspection of the sky region surrounding IRAS 09104+4109 using other X-ray catalogs confirms that a few low X-ray energy sources are contained within the PDS field of view. Of the 4 RASS objects found, one corresponds to IRAS 09104+4109 (0.1213 c/s) two are quasars at redshifts 0.936 (0.074 c/s) and 0.7325 (0.063 c/s) and one is a normal galaxy (0.111 c/s) (Bade et al. 1998). At higher energies (2-10 keV) we find a source in the HEAO-1 A1/A3 catalogues as well as in the ASCA-SIS database, which correspond to the IRAS source. We therefore conclude that the IRAS source is the dominant one in the 2-10 keV band and presumably also in the PDS energy range.

In what follows we model the broad-band BeppoSAX spectrum of the source, trying to reconcile the 0.1-10 keV data with the excess emission observed at higher energies and with the possible presence of a neutral iron line.

One possible explanation is in terms of a cluster hard tail (or a simple power-law emission) as detected by BeppoSAX in Coma and A2199 (Fusco-Femiano et al. 1999, Kaastra et al. 1999) superimposed on the cluster thermal component. However, we regard this possibility as highly unlikely for the following reasons: a) the hard tail photon index required by the data is much flatter ($\Gamma \leq 0.9$) than

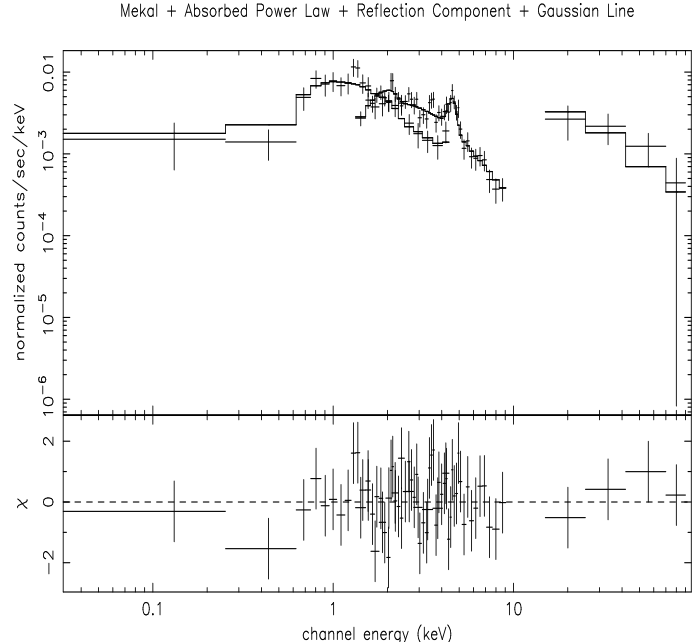


Fig. 3. Our best-fit model of the BeppoSAX X-ray spectrum of IRAS 09104+4109, in counts units. The model includes a MEKAL component ($kT=5.5$ keV and metal abundance $Z = 0.4 Z_{\odot}$) plus an absorbed power law ($N_H=7 \times 10^{24} \text{ cm}^{-2}$ and photon index $\Gamma=1.9$) with associated reflection component (reflected fraction $R = 0.2$) and neutral iron line (observed EW=1.3 keV); the residuals between the data and the model are plotted in the bottom panel.

dominates the 10-100 keV emission, while typically hard tails are responsible for 10-15% of the high energy output and c) this model would not explain the 6.4 keV iron line emission.

We therefore prefer the alternative explanation of an AGN deeply buried within a source immersed in the IC plasma. This requires that a high column density material ($N_H \geq 10^{24} \text{ cm}^{-2}$) absorbs the X-ray emission from the AGN, to avoid spoiling the good fit of the low energy data with the free-free model. Such high column densities are quite common in Seyfert 2 galaxies, as typically evidenced by high energy observations (Bassani et al. 1999a). We have therefore added an absorbed power-law plus a narrow gaussian line to take into account the obscured AGN emission. This results in a satisfactory fit ($\chi^2/\nu = 47.2/63$) and returns a column density of $N_H \simeq 6.7_{-1.3}^{+32.7} \times 10^{24} \text{ cm}^{-2}$ for a fixed photon index of 1.9. However, the EW of the 6.4 keV iron line would turn out to have an unrealistically high value ($>> 10$ keV), i.e the line must be extremely intense to survive the heavy absorption and to emerge above the cluster emission. It is therefore not compatible with pure transmission throughout the measured

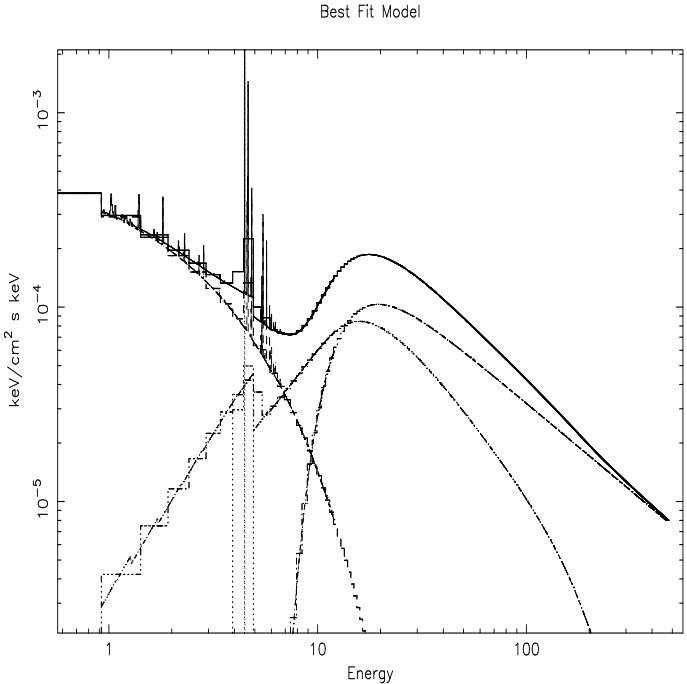


Fig. 4. Same best-fit model of the BeppoSAX X-ray spectrum of IRAS 09104+4109 as in Figure 3, but in physical units. The model includes an IC plasma component (the line with exponential cutoff at 5 keV), plus an absorbed power-law (line with low-energy cutoff at ~ 20 keV) with associated reflection component (line showing an edge at 4.44 keV) and neutral iron line (observed EW=1.3 keV, rest-frame EW=1.9 keV).

line must be produced in a different way, e.g. by reflection in the absorbing torus or in the surrounding material.

Consequently the data have been fitted using a more complex model assuming thermal emission from the cluster plus AGN emission, the latter including an absorbed power-law, to reproduce the X-ray flux transmitted through the absorbing torus, and a reflection spectrum with associated neutral iron line. Note that modelling the data with a pure reflection component cannot account for all of the high energy excess, so that both AGN components are required by our observations.

Obviously, given the limited statistics of our data, various parameters of this complex description (the primary power-law photon index [$\Gamma=1.9$], line energy [6.4 keV] and width [0] and cluster metal abundance [$Z=0.4$]) have to be fixed. In this case, good fits ($\chi^2/\nu=48-51/62$) are obtained if N_H is $\geq 5 \times 10^{24} \text{ cm}^{-2}$, and if the fraction R of the nuclear flux reflected over all directions is in the range $R=0.15-0.3$. For this choice of the parameters, the EW of the neutral Fe line is $\sim 1-2$ keV and the cluster temperature is 5.5 keV, quite consistent with the assumed metal abundance (see illustration in Figs. 3 and 4).

6. Discussion

IRAS 09104+4109 clearly shows a very complex phenomenology when observed in X-rays. Particularly informative about the dual nature of the source (including IC plasma emission at 0.1-7 keV and AGN emission above 7 keV) are our new BeppoSAX observations. In particular, the PDS data demonstrate the energetic dominance of AGN emission at the high energies, and add to independent evidence based on optical line spectroscopy and polarization measurements.

The best-fit parameters found for our cluster and AGN emissions are not "per se" unusual. In particular, the inferred AGN spectrum is similar to what is found in other highly absorbed Seyfert 2 galaxies, such as Mkn3, NGC4945, NGC6240 and the Circinus galaxy (Bassani et al. 1999b; Vignati 1999). Rather, what is unusual is to find the combined cluster/AGN phenomenon in a single source, and, for a Type-2 AGN like this, the absorption-corrected luminosity: 0.8 and $1.7 \times 10^{46} \text{ erg s}^{-1}$ in the 2-10 and 10-100 keV band respectively. These luminosities are well within the range of QSO observed values.

In spite of their limited statistics, and thanks to the very wide dynamic range in photon energy, BeppoSAX data are able to constrain the complex physical situation in the source. To get physically consistent solutions, our fitting procedure required two emission components in the AGN, one in transmission through the torus, the other in reflection to explain the neutral Fe line. The torus is expected to absorb low energy photons along obscured directions and, if N_H is large, to produce a reflection bump along unobscured directions. Indeed, while substantial absorption is confirmed, in particular, by the detection of the silicate $10 \mu\text{m}$ absorption feature by Taniguchi et al. (1997), anisotropic emission and scattering are clearly consistent with a variety of observations in the radio (the usual two-lobe structure) and optical (the highly polarized ionization cones detected by the HST imaging polarimetry, see Hines et al. 1999).

A rough match of the 2-10 keV luminosity with the OIII (corrected for reddening in the Narrow Line Region, Bassani et al. 1999a) and with IR emissions indicates L_X/L_{OIII} and L_X/L_{FIR} ratios of 18 and 0.3, i.e. fairly typical for Type-1 AGN (Bassani et al. 1999a, Mulchaey et al. 1994).

We have performed a detailed comparison of the observed hard X-ray and IR continua with predictions of radiative transfer codes (Granato, in preparation) accounting for (dust and photoelectric) absorption and scattering, including the anisotropy and incoherence of Compton scattering (particularly relevant for the X-rays). The codes have been tested against and found to be in agreement with Monte Carlo simulations.

We have then adopted for the gaseous torus in IRAS 09104+4109 the same geometry needed to reproduce the

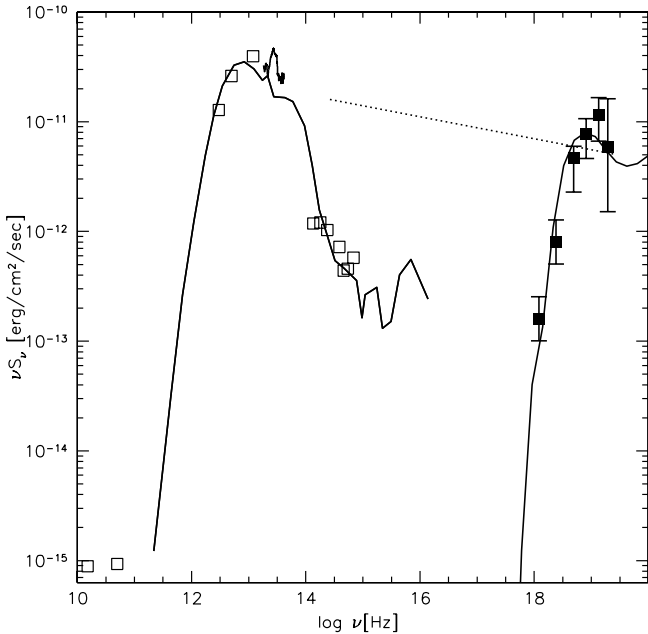


Fig. 5. The observed broad-band spectrum of the type-2 quasar IRAS 09104+4109 over 10 decades in photon energy. The cluster emission dominating the low X-ray energies has been omitted. The IR and hard X-ray spectra are fitted with the same self-consistent AGN model as described in Sect. 6. This includes a dusty torus structure around the central AGN and responsible for the IR emission (Granato et al. 1996), with the associated gas assumed to photoelectrically absorb and Compton scatter the X-ray photons. The dotted line shows a schematic fit to the average X-ray to IR spectrum of type-1 AGNs (Barcons et al. 1995) adopted by us to describe the AGN primary continuum. The continuous lines show the effect of the processing by the surrounding dusty torus. Data-points are from Taniguchi et al. (1997) for the IR and from BeppoSAX observations for the X-rays (two data points at 5 and 10 keV [$\log \nu = 18.08$ and $\log \nu = 18.36$] come from subtraction of the cluster contribution).

cones (Hines et al. 1999). Consistent with the results of our spectral analysis in Sect. 5, this geometry predicts a thick torus with opening angles of ~ 30 degrees observed with an angle of the symmetry plane with the line-of-sight of ~ 45 degrees. Then the predicted X-ray flux within the two frequencies ν_1 and ν_2 is given by:

$$F(\nu_1, \nu_2) = \frac{1}{4\pi d_L^2} L_{5\text{keV}}^{\text{QSO}} P_{\nu_{1e}, \nu_{2e}}(N_{\text{H}}) \quad (1)$$

where $\nu_e = \nu(1+z)$ and $L_{5\text{keV}}^{\text{QSO}}$ is the unobscured luminosity for a type-1 quasar, and $P_{\nu_{1e}, \nu_{2e}}(N_{\text{H}})$ is the thickness-dependent ratio between the flux emerging along lines of

unobscured directions at 5 keV, as derived from the solution of the radiative transfer equation.

As for the IR emission, the observed monochromatic flux at 60 μm is given by

$$F_{\nu}(60\mu\text{m}) = \frac{L_{\nu}^{\text{QSO}}(60\mu\text{m}/[1+z])}{4\pi d_L^2} (1+z) p_{60/[1+z]}(\tau_e, \Theta) \quad (2)$$

where $p_{60/[1+z]}(\tau_e, \Theta)$ is the ratio in the rest-frame between the monochromatic flux at $60/[1+z] \simeq 40$ μm emitted by the dusty torus with optical thickness τ_e along the line of sight (defined by the polar angle Θ) and the flux emitted along a typical unobscured direction. Combining the two above equations we get finally:

$$F(\nu_1, \nu_2) = \frac{F_{\nu}(60\mu\text{m}) R P_{\nu_{1e}, \nu_{2e}}(N_{\text{H}})}{p_{60/[1+z]}(\tau_e, \Theta) (1+z)} \quad (3)$$

where $R = L_{\nu}^{\text{QSO}}(5\text{keV})/L_{\nu}^{\text{QSO}}(60/[1+z]\mu\text{m})$.

Barcons et al. (1995) find an average $f_{\nu}(5\text{keV})/f_{\nu}(12\mu\text{m}) = 1.4_{-0.4}^{+1.1} \times 10^{-6}$ for a sample of 54 Seyferts 1 (error corresponding to 95% confidence). Adopting the mean IR SED for UVX quasars as in Elvis et al. (1994), this translates into an X-ray to IR ratio of $R \simeq 1.3 \times 10^{-6}$. Assuming $N_{\text{H}} = 6 \times 10^{24}$, $\tau_e = N_{\text{H}}/1.1 \times 10^{21}$, $\Theta = 45$ degrees, and for the observed monochromatic flux $F_{\nu}(60\mu\text{m}) = 550$ mJy, we obtain the hard X-ray spectrum reported in Fig. 5. The expected flux at 20-100 keV turns out to be $F(\nu_1, \nu_2) \simeq 8 \times 10^{-12}$ erg/cm²/sec, whereas the observed is $\simeq 10^{-11} \pm 0.3$ erg/cm²/sec.

Altogether, within the observed dispersion of the ratio of X-ray to IR flux for quasars, and within the uncertainties in the torus model geometry, the high-energy flux of IRAS 09104+4109 detected by BeppoSAX is consistent with emission by the same quasar which produces, via the reprocessing by the circumnuclear dust, the whole far-IR spectrum.

7. Conclusions

BeppoSAX observations of IRAS 09104+4109 provide evidence for the existence of a buried AGN and indicate that at least some objects classified as HyLIRGs can indeed harbour highly luminous X-ray sources, the long-sought high luminosity/redshift analogues of Seyfert2 galaxies.

In principle, this result could have implications for the long standing debate about the nature of the primary power source in ultraluminous IR galaxies and the related question of origin of the cosmological IR and X-ray backgrounds.

However, we have to consider the rather unique nature of this source, where the symbiosis of a bright IR quasar with a rich IC plasma including a massive cooling-flow is emphasized by the present BeppoSAX observations.

If we consider the rarity of luminous type-2 QSOs

F10214, IRAS F15307 and IRAS 23060, very rarely detected in X-ray surveys, e.g. RXJ13434+0001), then it is tempting to relate the peculiarity of IRAS 09104+4109 with the huge cooling-flow of $\sim 1000 M_{\odot}$ discovered by ROSAT HRI (Fabian & Crawford 1995). This condition of extremely fast mass accumulation could counter-balance the enormous radiation pressure by the quasar (which would otherwise quickly get rid of the obscuring envelope), hence favouring the persistence of a thick medium around it.

Acknowledgements. This research has made use of SAXDAS linearized and cleaned event files produced at the BeppoSAX Science Data Centre. Research partially supported by Italian Space Agency (ASI).

References

Barcons X., Franceschini A., De Zotti G., Danese L., Miyaji T., 1995, ApJ 455, 480

Bassani L., Dadina M., Maiolino R., et al. 1999a, ApJS 121, 473

Bassani L., Cappi M., Malaguti G., 1999b, Proceedings of 3rd INTEGRAL Workshop "The Extreme Universe", in press

Bade N., Engels D., Voges W., et al. 1998, A&AS 127, 145

Boella G., Butler R.C., Perola G.C., Piro L., Scarsi L., Bleeker J.A.M. 1997a, A&AS 122, 299

Boella G., Chiappetti L., Conti G., et al. 1997b, A&AS 122, 327

Chiappetti L., Dal Fiume D., 1997, in Scarsi L., Maccarrone M. (eds.), Proceedings of the 5th International Workshop on Data Analysis in Astronomy

Elvis M., Wilkes B., McDowell J., et al., 1994, ApJS 95 1

Evans A.S., Sanders D.B., Cutri R. M. et al. 1998, ApJ 506, 205

Fabian A.C., Shioya Y., Iwasawa K., et al., 1994a, ApJ 463, L51

Fabian A.C., Crawford C.S., Edge A.C., Mushotzky R.F. 1994b, MNRAS 267, 779

Fabian A.C., Crawford C.S. 1995, MNRAS 274, L63

Fiore F., Guainazzi M., Grandi P. 1999, "Handbook for NFI spectral analysis" (<http://www.tesre.bo.cnr.it/SAX/software/>)

Frontera F., Costa E., Dal Fiume D., et al. 1997, A&AS 122, 357

Fusco-Femiano R., Dal Fiume D., Ferretti L., et al. 1999, ApJ 513, L21

Genzel R., Lutz D., Sturm E., et al., 1998, ApJ 498, 579

Granato G.L., Danese L., Franceschini A., 1996, ApJL 460, L11

Guainazzi M., Perola C., Matt G. et al., 1999, A&A 346, 407

Guainazzi M. and Matteuzzi L., 1997, BeppoSAX SDC technical Report , TR-011

Hines D.C., Wills B.J., 1993, ApJ 415, 82

Hines D.C., Schmidt G.D., Wills B.J., Smith P.S., Sowinski L.G. 1999 ApJ 512, 145

Kaastra J.S., Lieu R., Mittaz J.P.D., et al. 1999 ApJ Letters, in press

Kleinmann S.G., Hamilton D., Keel W.C. et al., 1988, ApJ

Leahy D.A., Creighton J., 1993, MNRAS 263, 314

Mulchaey J.S., Koratkar A., Ward M.J., et al. 1994, ApJ 436, 587

Murphy E.D., Lockman F.J., Laor A., Elvis M. 1996, ApJS 105, 369

Ogasaka Y., Inoue H., Brandt W.N. et al., 1997, PASJ 49, 1790

Parmar A.N., Martin D.D.E., Baudz M., et al., 1997, A&AS 122, 309

Taniguchi Y., Sato Y., Kawara K., Murayama T., Mouri H., 1997, A&A 318, L1

Vignati, 1999, Laurea thesis, Milano Italy